Development 136, 2223-2234 (2009) doi:10.1242/dev.034603

MSP and GLP-1/Notch signaling coordinately regulate actomyosin-dependent cytoplasmic streaming and oocyte growth in *C. elegans*

Saravanapriah Nadarajan[1,*], J. Amaranath Govindan[1,*], Marie McGovern[2], E. Jane Albert Hubbard[2] and David Greenstein[1,†]

Fertility depends on germline stem cell proliferation, meiosis and gametogenesis, yet how these key transitions are coordinated is unclear. In *C. elegans*, we show that GLP-1/Notch signaling functions in the germline to modulate oocyte growth when sperm are available for fertilization and the major sperm protein (MSP) hormone is present. Reduction-of-function mutations in *glp-1* cause oocytes to grow abnormally large when MSP is present and $G\alpha_s$-adenylate cyclase signaling in the gonadal sheath cells is active. By contrast, gain-of-function *glp-1* mutations lead to the production of small oocytes. Surprisingly, proper oocyte growth depends on distal tip cell signaling involving the redundant function of GLP-1 ligands LAG-2 and APX-1. GLP-1 signaling also affects two cellular oocyte growth processes, actomyosin-dependent cytoplasmic streaming and oocyte cellularization. *glp-1* reduction-of-function mutants exhibit elevated rates of cytoplasmic streaming and delayed cellularization. GLP-1 signaling in oocyte growth depends in part on the downstream function of the FBF-1/2 PUF RNA-binding proteins. Furthermore, abnormal oocyte growth in *glp-1* mutants, but not the inappropriate differentiation of germline stem cells, requires the function of the cell death pathway. The data support a model in which GLP-1 function in MSP-dependent oocyte growth is separable from its role in the proliferation versus meiotic entry decision. Thus, two major germline signaling centers, distal GLP-1 activation and proximal MSP signaling, coordinate several spatially and temporally distinct processes by which germline stem cells differentiate into functional oocytes.

KEY WORDS: MSP signaling, Notch signaling, Meiosis, Meiotic maturation, Germline stem cell, Cytoplasmic streaming, *Caenorhabditis elegans*

INTRODUCTION

A key question in developmental biology is how conserved intercellular signaling pathways work in concert to generate cellular differentiation programs. Here we present evidence that two conserved signaling pathways, the classical Notch pathway and the more recently described major sperm protein (MSP) signaling pathway (Miller et al., 2001), coordinate the program by which germline stem cells develop into functional oocytes in the nematode *C. elegans*.

The *C. elegans* hermaphrodite gonad is a paradigm for studying intercellular signaling during development (Schedl, 1997). The somatic distal tip cell (DTC) caps the distal end of each gonad arm (see Fig. S1 in the supplementary material) and maintains a distal population of undifferentiated germ cells. Removal of the DTC causes all germ cells to enter meiosis (Kimble and White, 1981). The GLP-1/Notch receptor functions in the germline (Austin and Kimble, 1987; Austin and Kimble, 1989; Yochem and Greenwald, 1989) and is activated by interaction with the DSL family ligand LAG-2 expressed in the DTC (Henderson et al., 1994; Tax et al., 1994). GLP-1 functions together with LAG-1, which encodes a CSL transcription factor (Christensen et al., 1996). GLP-1 is thought to regulate transcription of genes that promote proliferation and/or inhibit meiotic entry (Hansen and Schedl, 2006; Kimble and Crittenden, 2007).

[1]Department of Genetics, Cell Biology and Development, University of Minnesota, 6-160 Jackson Hall, 321 Church Street SE, Minneapolis, MN 55455, USA. [2]New York University School of Medicine, Skirball Institute of Biomolecular Medicine, 4th Floor, Lab 7, 540 First Avenue, New York, NY 10016, USA.

*These authors contributed equally to this work
†Author for correspondence (e-mail: green959@umn.edu)

Accepted 22 April 2009

The PUF ('Pumilio and FBF') RNA-binding proteins FBF-1 and FBF-2 act in the proliferation versus meiotic entry decision (Crittenden et al., 2002; Hansen et al., 2004) and also play a crucial role in germline sex determination by promoting the sperm-to-oocyte switch (Zhang et al., 1997). FBF-2 levels depend on GLP-1 signaling, and the *fbf-2* 5′-flanking region contains LAG-1 binding sites that are functional in vitro, implicating *fbf-2* as a direct GLP-1 target (Lamont et al., 2004). GLP-1 signaling negatively regulates the activity of the GLD-1 and GLD-2 post-transcriptional gene regulatory pathways, which control meiotic entry (Hansen and Schedl, 2006; Kimble and Crittenden, 2007).

With the exception of the end stages of gametogenesis, *C. elegans* germ cells maintain connection to a core of cytoplasm, the contents of which flow into developing oocytes (Hirsh et al., 1976; Wolke et al., 2007). In adult hermaphrodites, germ cells that exit pachytene either differentiate as oocytes or undergo apoptosis (Gumienny et al., 1999). Female meiotic germ cells destined for apoptosis might function as nurse cells that contribute their contents to the cytoplasmic core and thus to developing oocytes (Gumienny et al., 1999; Jaramillo-Lambert et al., 2007). However, actomyosin-dependent cytoplasmic streaming that drives oocyte growth in the loop region of the gonad (see Fig. S1 in the supplementary material) occurs normally in the absence of apoptosis (Wolke et al., 2007). Oocytes in the loop region grow primarily by receiving flow from the core cytoplasm (Wolke et al., 2007), and yolk uptake in the most proximal oocytes also contributes (Grant and Hirsh, 1999; Wolke et al., 2007). The pathways that control incomplete cytokinesis in the distal germline, and that promote cellularization of developing oocytes in the proximal germline, are incompletely understood. Several genes with important functions in cytokinesis are required for oocyte cellularization, including *mlc-4*, *mel-11* and *cyk-1*, which encode the regulatory light chain of non-muscle myosin, a myosin

phosphatase regulatory subunit and an actin regulator, respectively (Piekny and Main, 2002; Shelton et al., 1999; Swan et al., 1998). The anillin ANI-2 is required for developing oocytes to maintain their connection to the core cytoplasm (Maddox et al., 2005). How intercellular signaling regulates oocyte growth and cellularization has not been extensively addressed, although prior work implicates the PTP-2 protein tyrosine phosphatase and MPK-1 mitogen activated protein kinase (MAPK) in oocyte growth control in *C. elegans* (Gutch et al., 1998; Lee et al., 2007).

In the accompanying article (Govindan et al., 2009), we show that MSP signaling triggers the cytoplasmic flows that drive oocyte growth. When MSP is absent, as in mutant hermaphrodites that do not produce sperm (e.g. *fog* mutant females), cytoplasmic streaming and oocyte production cease. $G\alpha_s$-adenylate cyclase signaling in the gonadal sheath cells is required for all the described MSP responses in the germline, including cytoplasmic streaming (Govindan et al., 2009). Thus, MSP signaling via the gonadal sheath cells coordinately regulates the production, growth and meiotic maturation of oocytes. Here, we provide evidence that DTC signaling via GLP-1 regulates MSP-dependent cytoplasmic streaming, oocyte growth and cellularization. Thus, two major signaling centers in the adult hermaphrodite gonad, GLP-1 distally and MSP proximally, function both separately in germ cell fate (mitotic versus meiotic) and meiotic maturation, respectively, and in opposition to regulate the growth of germ cells into functional oocytes.

MATERIALS AND METHODS

C. elegans strains, genetics and phenotypic analysis

C. elegans strains used are available on request. Phenotypic analysis was performed as described in the accompanying article (Govindan et al., 2009). Worms were cultured at 20°C, with the following exceptions: temperature sensitive (ts) strains were grown at 15°C and analyzed at 25°C; Looc phenotypes and cytoplasmic flows were analyzed at 25°C; and RNAi feeding was at 25°C, unless stated otherwise. Oocyte volumes were estimated (McCarter et al., 1999) and gonad arms were scored as having a Looc phenotype if oocyte volumes were at least 20% larger than that of the –1 oocyte in the wild type. In *glp-1* gain-of-function mutants, oocytes were scored as small if their volumes were at least 30% less than wild type. When L4-stage larvae were transferred from 15°C to 25°C and oocyte volumes were measured 16 hours later, the –1 oocyte in the wild type was 16,532±3311 μm^3 (n=25), whereas in *glp-1(tn777ts)*, we observed a 63% increase in average volume (26,948±9316 μm^3; n=17; P<0.0001). Primer sequences used are available on request. An *apx-1* RNAi feeding clone (pGC304) was constructed as follows: *apx-1* cDNA was PCR-amplified from a cDNA library (Invitrogen, Carlsbad, CA, USA), the PCR product was subcloned into L4440 and DNA sequencing was used to confirm the identity of the clone. For generating dsRNA for *mlc-4(RNAi)* using the injection method, the template was first-strand N2 cDNA.

Mosaic analysis

glp-1 mosaics were sought using DG2545 *glp-1(tn777ts) ncl-1(e1865) unc-36(e251); qDp3*; ~15,000 non-Unc L4 larvae were transferred to 25°C and scored for the Looc phenotype 16 hours later. Mosaics were scored using the Ncl phenotype (Hedgecock and Herman, 1995); germline mosaics were scored by progeny testing.

DTC ablations and oil injections

Laser ablations were conducted on L4 and young-adult hermaphrodites on an Olympus BX60 microscope using DIC optics and a 100× (NA 1.4) objective lens. Animals were analyzed by DIC microscopy 12 hours after laser microsurgery to determine whether the DTC nucleus was absent. Successfully ablated animals were scored for the Looc phenotype 30 hours after ablation. These gonad arms were then stained with DAPI, which revealed that all distal germ cells had differentiated and in no case was the DTC nucleus observed, confirming the prior assessment of the DTC ablation. Laser-treated animals for which the DTC nucleus was still present 12 hours after laser microsurgery often had damaged DTC cell bodies. These animals were scored 30 hours after ablation, and did not have a Looc phenotype. Heavy paraffin oil (~1-4 pl, Sigma-Aldrich, St Louis, MO, USA) was injected within the first ten rows of the distal germ cells of young adult hermaphrodites (~12 hours post L4) using a Narshige micromanipulator on a Zeiss Axiovert-35 microscope.

Fluorescence microscopy

A Zeiss motorized Axioplan 2 microscope with a 63× PlanApo (NA 1.4) objective lens and an apotome adaptor was employed for fluorescence microscopy. Fluorescence images were acquired with an AxioCam MRm camera and AxioVision acquisition software. Anti-PSer19rMLC antibodies (Cell Signaling Technology, Danvers, MA, USA) and rhodamine-phalloidin (Sigma-Aldrich, St Louis, MO, USA) were used at 1:200 and 0.5 μM, respectively. SYTO 12 (Invitrogen, Carlsbad, CA, USA) staining was used to examine apoptosis in the germline (Gumienny et al., 1999).

RESULTS

GLP-1/Notch activity controls oocyte growth

To elucidate the mechanisms that coordinate oocyte growth and meiotic maturation, we undertook a forward genetic screen for mutants that produce large oocytes (*looc* mutants; *C. elegans* strains used are available on request). As oocytes are generated in the adult stage, we screened for temperature sensitive (ts) mutations to bypass earlier *looc* gene requirements. Surprisingly, we recovered two *glp-1* alleles (*tn231* and *tn777*) as *looc* mutations (Fig. 1A,B).

Several lines of evidence establish that *glp-1* activity negatively regulates oocyte growth. Recessive reduction-of-function (rf) mutations in *glp-1* can confer the Looc phenotype. The *tn777ts looc* mutation maps to the same genetic interval as *glp-1* and fails to complement the *glp-1(q158)* null allele (Austin and Kimble, 1987) for the Looc and Glp phenotypes, depending on when the heterozygotes are transferred to the non-permissive temperature (i.e. L4- and L1-stage larvae, respectively; *glp-1* null alleles produce only four to eight germ cells that differentiate as sperm). All tested *glp-1(ts)* alleles exhibited a Looc phenotype (Fig. 1A), except for *glp-1(e2142ts)*, which specifically interferes with *glp-1* function in the embryo (Priess et al., 1987; Kodoyianni et al., 1992). The independently isolated alleles *tn231* and *tn777* have the same G to A base change as *glp-1(bn18)*, which causes an alanine to threonine amino acid substitution (A1034T) in one of the intracellular cdc10/SWI6 motifs. Furthermore, *glp-1(RNAi)* in a wild-type background produced a Looc phenotype (47% penetrance; n=78), whereas control RNAi treatments had no effect on oocyte size. Finally, the weak gain-of-function *glp-1* alleles, *ar202* (Fig. 1B) and *ar218*, produced smaller oocytes than the wild type at a penetrance of 50.6% (n=166; *ar202*) and 42% (n=147; *ar218*).

Genetic mosaic analysis establishes that *glp-1* function is required in the germline for normal oocyte growth control; losses of *glp-1(+)* function within the germline lineages (P3 and P4) were sufficient to cause a Looc phenotype (n=6). We obtained one P3 loss and five P4 losses with a Looc phenotype. Furthermore, *glp-1(RNAi)* in the *rrf-1(pk1417)* somatic-RNAi-deficient background (Sijen et al., 2001) produced a Looc phenotype (50% penetrance; n=101).

GLP-1 signaling regulates MSP-dependent oocyte growth

The *looc* mutations fall into two classes: sperm-dependent *looc* mutants produce large oocytes only in the presence of sperm; and sperm-independent *looc* mutants produce large oocytes constitutively. *glp-1* alleles (*tn231* and *tn777*) are sperm-dependent *looc* mutations (Fig. 1A,B). Several observations show that the

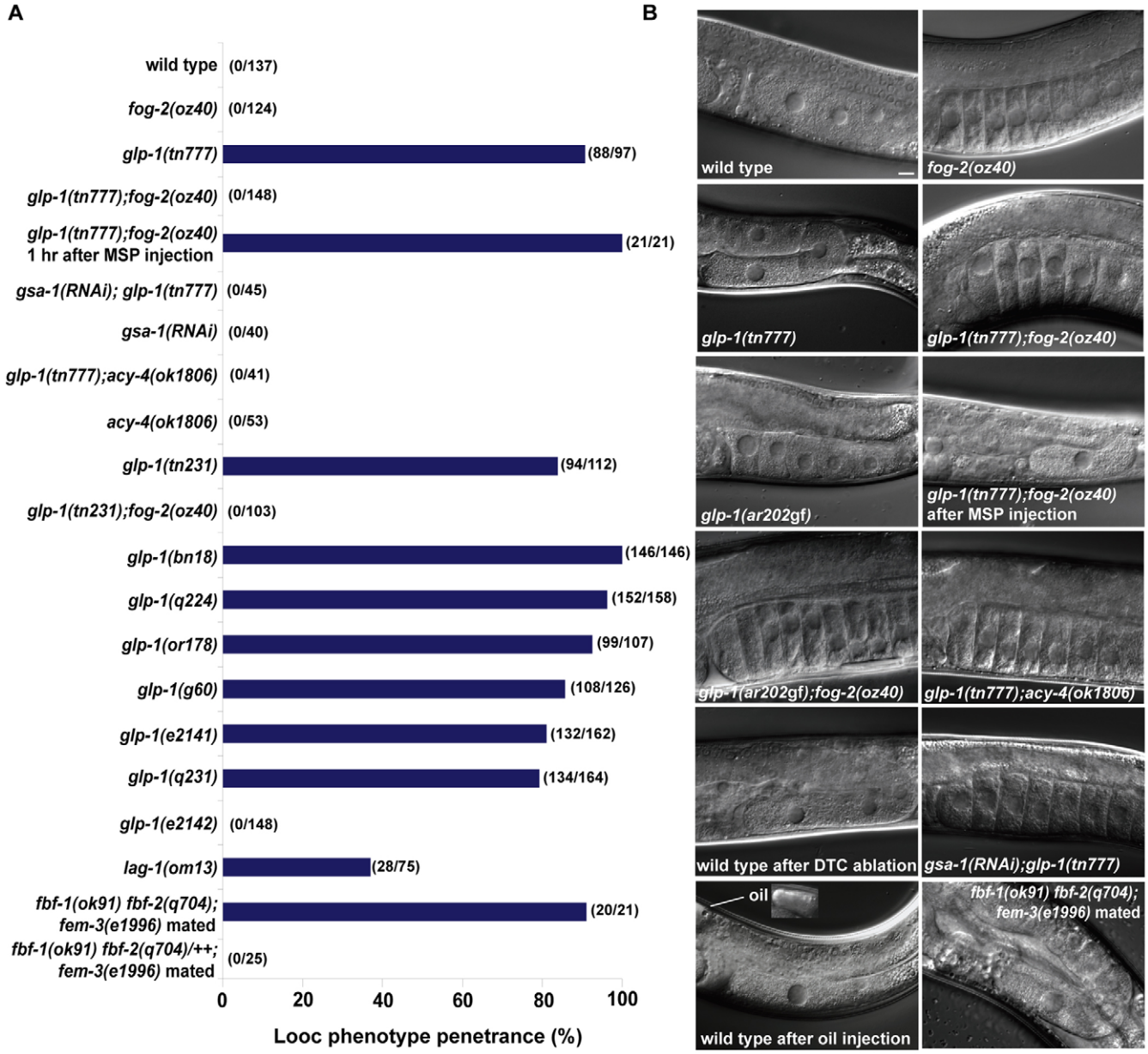

Fig. 1. GLP-1 regulates MSP-dependent oocyte growth. (**A**) Penetrance of the Looc phenotype in *glp-1, fbf* and *lag-1* mutants, measured 16 hours post-L4 at 25°C in hermaphrodite or female backgrounds. In this and subsequent figures, gonad arms were scored as having a Looc phenotype if oocyte volumes were at least 20% larger than that of the –1 oocyte in the wild type. (**B**) DIC images showing oocyte size phenotypes in *glp-1* mutants, and after DTC ablations or distal oil injection (see Table 1). Inset shows the distal region in which oil was injected. Scale bar: 10 μm.

glp-1 Looc phenotype is dependent on the presence of MSP. *glp-1(tn777); fog-2(oz40)* females did not exhibit a Looc phenotype, unless mated (Fig. 1A,B). Mating induced the Looc phenotype rapidly, within 15 minutes in 51% of the gonad arms (Fig. 2; n=74). By 15 minutes after mating of *glp-1(tn777); fog-2(oz40)* females, Looc oocytes in the loop region (at positions –9 to –11) had an average volume of 19,104±4389 μm^3 (n=13), which was 68% larger (P<0.0001) than the volume (11,341±3114 μm^3; n=17) of oocytes from the same position of mated *fog-2(oz40)* females. Injection of MSP into the uterus of *glp-1(tn777); fog-2(oz40)* females was sufficient to cause a Looc phenotype in all gonad arms after 1 hour (Fig. 1A,B). MSP injection into *glp-1(tn777); fog-2(oz40)* females could also produce a Looc phenotype within 15 minutes, although MSP injection was substantially less efficient than mating at this early timepoint (S.N. and D.G., unpublished). The small oocyte phenotype in *glp-1(ar202gf)* was also sperm dependent (Fig. 1B; n=52). In the accompanying article, we show that Gα_s-adenylate cyclase signaling in the gonadal sheath cells is required for all described MSP-dependent responses in the germline, including cytoplasmic streaming that drives oocyte growth (Govindan et al., 2009). Thus we investigated the effect of an *acy-4(lf)* mutation and *gsa-1(RNAi)* on the *glp-1* Looc phenotype. We found that *acy-4(lf)* and *gsa-1(RNAi)* completely suppressed the *glp-1* Looc phenotype (Fig. 1A,B). These results indicate that the level of *glp-1* signaling controls oocyte size in a manner that is dependent on MSP signaling.

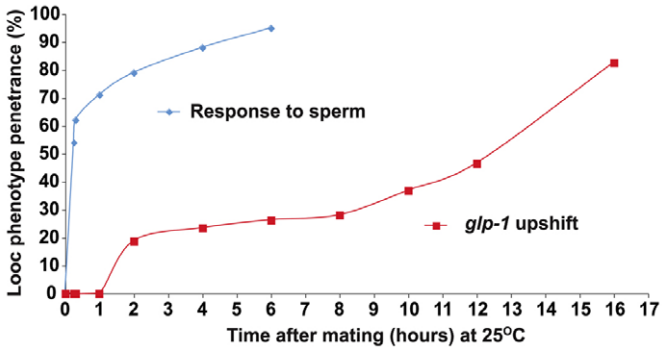

Fig. 2. Time-course analysis of sperm-dependence and *glp-1* contributions to oocyte growth. To examine the sperm response, *glp-1(tn777ts); fog-2(oz40)* L4-stage larvae were transferred to 25°C for 24 hours and then mated with CB4855 wild-type males. The Looc penetrance increases rapidly after mating (blue line). To examine the *glp-1* requirement, *glp-1(tn777ts); fog-2(oz40)* day-1 adult females were mated at 15°C and then transferred to 25°C. The Looc penetrance was measured at different times after mating with CB4855 males (red line).

To determine the temporal requirement for *glp*-1 in MSP-dependent oocyte growth, we conducted a series of time-course studies (Fig. 2). First, we analyzed the temporal requirement for sperm for the generation of the *glp-1* Looc phenotype. We transferred L4-stage *glp-1(tn777); fog-2(oz40)* females to the non-permissive temperature to inactivate *glp-1*, allowed the females to develop to adulthood and then mated them with CB4855 wild-type males. We observed a rapid increase in the penetrance of the Looc phenotype after mating, first observing the phenotype in approximately 50% of the animals after 15 minutes (Fig. 2, blue line). Because the response to sperm is rapid, and evidently the effects of *glp-1* depletion are slower, we were able to assess separately the contribution of *glp-1* to the control of oocyte size. To examine the *glp-1* requirement, day-1 adult *glp-1(tn777); fog-2(oz40)* females were mated with CB4855 males at 15°C, and immediately transferred to 25°C after insemination. In this experiment, we first observed the Looc phenotype after 2 hours in approximately 20% of the animals (Fig. 2, red line). The penetrance of the Looc phenotype slowly rose over 16 hours. By comparison, it took approximately 8 hours for all germline stem cells to enter meiosis after temperature shift of *glp-1(tn777ts)* mutants (*n*=16), and all gonad arms still contained undifferentiated germ cells 4 hours after temperature shift (*n*=22). At this 4 hour timepoint, mitotic figures were observed in five of 22 germlines. The duration of meiotic S phase is approximately 3 hours, and the length of meiotic prophase during oogenesis is approximately 54-60 hours (Jaramillo-Lambert et al., 2007). Thus, the *glp-1* Looc phenotype is first observed before a substantial number of germ cells enter meiosis. Furthermore, it might have been that the *glp-1(ts)* Looc phenotype resulted from an increase in pachytene cells, which could contribute their cytoplasm to growing oocytes; however, *glp-1(ts)* hermaphrodites and females actually possessed fewer pachytene cells than the wild type (see Table S1 in the supplementary material). Germline stem cells inappropriately differentiated upon upshift of *glp-1(ts)* hermaphrodites and females (see Fig. S2 in the supplementary material), but the Looc phenotype was only seen when sperm were present. These studies on the temporal and sperm dependence of the Looc phenotype suggest that function of *glp-1* in oocyte growth is separable from its role in the proliferation versus meiotic entry decision. Additional evidence supporting this idea is presented and discussed further below.

MSP-dependent oocyte growth requires distal tip cell signaling

To investigate how *glp-1* functions to restrict oocyte growth, we examined downstream components of the pathway. We found that a hypomorphic mutation in the CSL/suppressor of hairless transcription factor *lag-1(om13ts)* also exhibited a Looc phenotype (Fig. 1A), confirming that this function is mediated through a

Table 1. Distal tip cell signaling regulates oocyte growth

Background	RNAi/treatment*	Looc penetrance (%)	*n*
Wild type	Control	0	87
Wild type	*lag-2*	19.3	98
Wild type	*apx-1*	8.3	120
Wild type	*apx-1; lag-2*	39.7	68
lag-2(q420ts)	Control	8.6	69
lag-2(q420ts)	*lag-2*	54.2	70
lag-2(q420ts)	*apx-1*	63.0	49
lag-2(q420ts)	*apx-1; lag-2*	78.9	57
Wild type	DTC ablation†	100	10
Wild type	Germ cell ablation‡	0	5
Wild type	Distal oil injection§	90.9	11
Wild type	Control injection§,#	0	11
fog-2(oz40), unmated	Distal oil injection§	0	11
fog-2(oz40), mated	Distal oil injection§	88.9	9
glp-1(ar202gf)	Distal oil injection§,**	100	5
glp-1(ar202gf)	Control injection§	0	17

*RNAi feeding was conducted at 15°C and the F1 progeny were transferred to 25°C at L4. *apx-1(RNAi) lag-2(RNAi)* on *lag-2(q420ts)* at 25°C results in a penetrant sterile phenotype (58.6%) in which reduced numbers of germ cells and no oocytes are produced. The Looc penetrance was measured 16 hours post-L4 in animals (*n*) that had oocytes; additional sterile animals with reduced numbers of germ cells and no oocytes are not included. These sterile animals represented 15.0% and 58.6% of the total, an additional 12 and 81 animals in the *lag-2(RNAi) apx-1(RNAi)* in the wild-type and *lag-2(q420ts)* backgrounds, respectively.
†An additional 18 animals were subjected to laser microsurgery; DIC microscopy established that the DTC was damaged but not ablated. These animals did not exhibit a Looc phenotype at 30 hours.
‡Five distal germ cells were ablated as a control.
§Animals were scored for the Looc phenotype 24 hours after injection or mating.
#Uninjected arms served as the control.
**An additional injected gonad arm exhibited a proximal proliferation phenotype and did not produce oocytes.

canonical Notch signaling pathway. We next analyzed the role of *fbf-1* and *fbf-2* in oocyte growth. Because *fbf-1(ok91) fbf-2(q704)* mutants have masculinized germlines, we analyzed *fbf-1(ok91) fbf-2(q704); fem-3(e1996m+z–)* females that produce oocytes (Thompson et al., 2005). We observed that 95% of mated *fbf-1(ok91) fbf-2(q704); fem-3(e1996m+z–)* females exhibited a Looc phenotype (Fig. 1A,B). By contrast, mated *fbf-1(ok91) fbf-2(q704)/++; fem-3(e1996m+z–)* heterozygotes or unmated *fbf-1(ok91) fbf-2(q704); fem-3(e1996m+z)* females did not exhibit a Looc phenotype (Fig. 1A; S.N. and D.G., unpublished). These results suggest that *fbf-1 fbf-2* activity is also required for MSP-dependent restriction of oocyte growth.

GLP-1 activity in the distal germline is activated by interaction with the DSL family ligand LAG-2 that is expressed in the DTC (Lambie and Kimble, 1991; Henderson et al., 1994). To test whether the regulation of oocyte growth by GLP-1 requires DTC signaling, we ablated the DTC by laser microsurgery in the late L4 or young adult stage in wild-type hermaphrodites. DTC ablation invariably produced a Looc phenotype after 30 hours (*n*=10; Fig. 1B; Table 1). Ablation of five germ cells within the proliferative zone did not generate a Looc phenotype (Table 1). Surprisingly, reducing *lag-2* function using the *q420ts* hypomorphic mutation or RNAi did not cause a highly penetrant Looc phenotype [9% Looc for control RNAi in *lag-2(q420ts)*; 19% Looc, *n*=98 for *lag-2(RNAi)* in wild-type hermaphrodites; Table 1], suggesting the presence of a DTC function redundant with LAG-2. APX-1 is a DSL ligand that is closely related to LAG-2 (Mello et al., 1994). An *apx-1* reporter is expressed in the DTC starting in the third larval stage (Fig. 3A-D). We found that *apx-1* contributes to the germline proliferation versus meiotic entry decision (Fig. 3E; see Tables S2 and S3 in the supplementary material). Specifically, we performed feeding RNAi experiments at 20°C and scored for Glp-1-like sterility (in which all germ cells display nuclear morphology consistent with meiotic prophase or gametogenesis). When *lag-2* or *apx-1* were depleted by RNAi we did not observe a Glp-1-like sterile phenotype (Fig. 3E). However, *apx-1(RNAi)* increased the penetrance with which a Glp-1 sterile phenotype was observed in *lag-2(q420ts)* adult hermaphrodites (Fig. 3E). Similarly, *lag-2(RNAi)* in an *apx-1(or3)* background produced a Glp-1-like sterile phenotype (38% penetrance), whereas a Glp-1-like sterile phenotype was not observed following the control RNAi in the *apx-1(or3)* background (Fig. 3E). These data suggest that, whereas the DTC-expressed LAG-2 activates GLP-1 in early larval stages, APX-1 and LAG-2 are redundant ligands for GLP-1 after *apx-1* DTC expression commences, and both contribute to GLP-1 activation thereafter.

To examine whether LAG-2 and APX-1 also act redundantly for oocyte growth control, we conducted RNAi in wild-type and *lag-2(q420ts)* backgrounds (Table 1). RNAi feeding was conducted at 15°C and the F1 progeny were transferred to 25°C at the L4 stage. We found that *apx-1* is also redundant with *lag-2* for oocyte growth: the penetrance of the Looc phenotype was elevated when both *lag-2* and *apx-1* were reduced [40% Looc in the wild-type background; 79% in the *lag-2(q420ts)* background; Table 1] and more closely resembled that observed after DTC ablation. Therefore, the GLP-1 DTC ligands LAG-2 and APX-1 are redundantly required for normal oocyte growth control (Table 1).

Where in the germline does *glp-1* function to regulate oocyte growth? Membrane-localized GLP-1 is enriched in the distal proliferative zone (Crittenden et al., 1994), but the distribution of the transcriptionally active form, GLP-1-INTRA, is unknown. Previously, oil injections were used to demonstrate that oocytes in the loop region and the proximal gonad generate the forces driving cytoplasmic streaming (Wolke et al., 2007). We reasoned that if

D

Gonad development	stage	% animals with DTC expression	n
4 cell gonad	earlyL1	0	28
>4-cell gonad; no SPG	L1-L2	0	15
SPG formed	L2/L3	16	69
Arms extending	earlyL3	96	47
Arms extending	midL3	98	81
Arms turning dorsal	lateL3	100	13
Arms turning centrifugal	L3/L4	100	11
Arms ¾ reflexed	L4	100	24
Arms fully reflexed	Adult	100	47

E

Background	RNAi	Glp(%)	n
wild type	control	0	307
wild type	*lag-2*	0	38
wild type	*apx-1*	0	94
lag-2(q420ts)	control	35	50
lag-2(q420ts)	*apx-1*	58	26
apx-1(or3)	control	0	40
apx-1(or3)	*lag-2*	38	42

Fig. 3. An *apx-1* reporter is expressed in the DTC after the L2 stage, and APX-1 functions redundantly with LAG-2 to promote germline proliferation. (**A-C**) *apx-1* expression was examined using an *apx-1* promoter::*lacZ* fusion (Chen and Greenwald, 2004) in the early L1 stage (A, 1 hour), in the early L3 stage (B, 21 hours) and in the L4 stage (C, 31 hours). All times are post-hatch at 25°C; white arrow indicates the DTC. White bar underscores the gonad in A. (**D**) Time-course analysis of *apx-1::lacZ* expression in the DTC. The somatic primordium of the gonad (SPG) forms at the beginning of the L3 stage. (**E**) Penetrance of Glp-1-like phenotype (all germ cells in a gonad arm displaying nuclear morphology consistent with meiotic prophase or gametogenesis). Synchronous L1 larvae were transferred to RNAi plates, and fixed and stained with DAPI ~50 hours later at 20°C. Control RNAi is L4440 vector. In addition to scoring the Glp-1-like sterile phenotype, less severe phenotypes were also observed (for a classification of all phenotypes and a complete description of the RNAi conditions, see Table S2 in the supplementary material).

glp-1 activation in the distal gonad regulates oocyte growth, then distal oil injections might interfere with the proximal transport of GLP-1-INTRA and/or downstream targets of GLP-1 signaling. To test this possibility, we injected a small volume of oil into the distal proliferative zone of adult wild-type hermaphrodites and analyzed oocyte growth at various timepoints. Although this operation disrupted nuclear morphology of distal germ cells, germ cells in the transition and pachytene zones appeared morphologically normal, and the gonad arm retained fertility for at least 24 hours (see Fig. S3 in the supplementary material). Following distal oil injections, we observed a Looc phenotype in 10 of 11 injected gonad arms by 24 hours after injection (Fig. 1B; Table 1). The uninjected gonad arms were not affected (Table 1). Oil injections into unmated *fog-2(oz40)* females did not cause a Looc phenotype (n=11), unless they were mated afterwards, in which case eight of nine mated females exhibited a Looc phenotype (Table 1). If *glp-1* functions in the distal proliferative zone to regulate oocyte growth proximally, we reasoned that distal oil injections would suppress the small oocyte phenotype observed in *glp-1(ar202gf)* mutants. Indeed, this was the case in five of five injected animals. Furthermore, all these animals exhibited a Looc phenotype, indicating that not only was the *glp-1(ar202gf)* phenotype suppressed, but there was a *glp-1(rf)* phenocopy. These results suggest that *glp-1(+)* function is needed in the distal gonad for oocytes to grow properly.

GLP-1 regulates actomyosin-dependent cytoplasmic streaming and oocyte cellularization

In the accompanying article, we show that MSP signaling is required to sustain the actomyosin-dependent cytoplasmic streaming that drives oocyte growth (Govindan et al., 2009). To address the mechanism by which GLP-1 signaling controls MSP-dependent oocyte growth, we measured cytoplasmic streaming rates in the loop region. We observed that mutations in *glp-1* caused a significant elevation in cytoplasmic streaming (Fig. 4A; see Movies 1 and 2 in the supplementary material). By contrast, the weak gain-of-function *glp-1* alleles *ar202* and *ar218* exhibited reduced cytoplasmic streaming compared with the wild type (Fig. 4A). In the wild type, cytoplasmic streaming begins in the pachytene region and flows are not observed within the distal third of the gonad arm (Wolke et al., 2007). Because distal germ cells enter meiosis upon upshift of

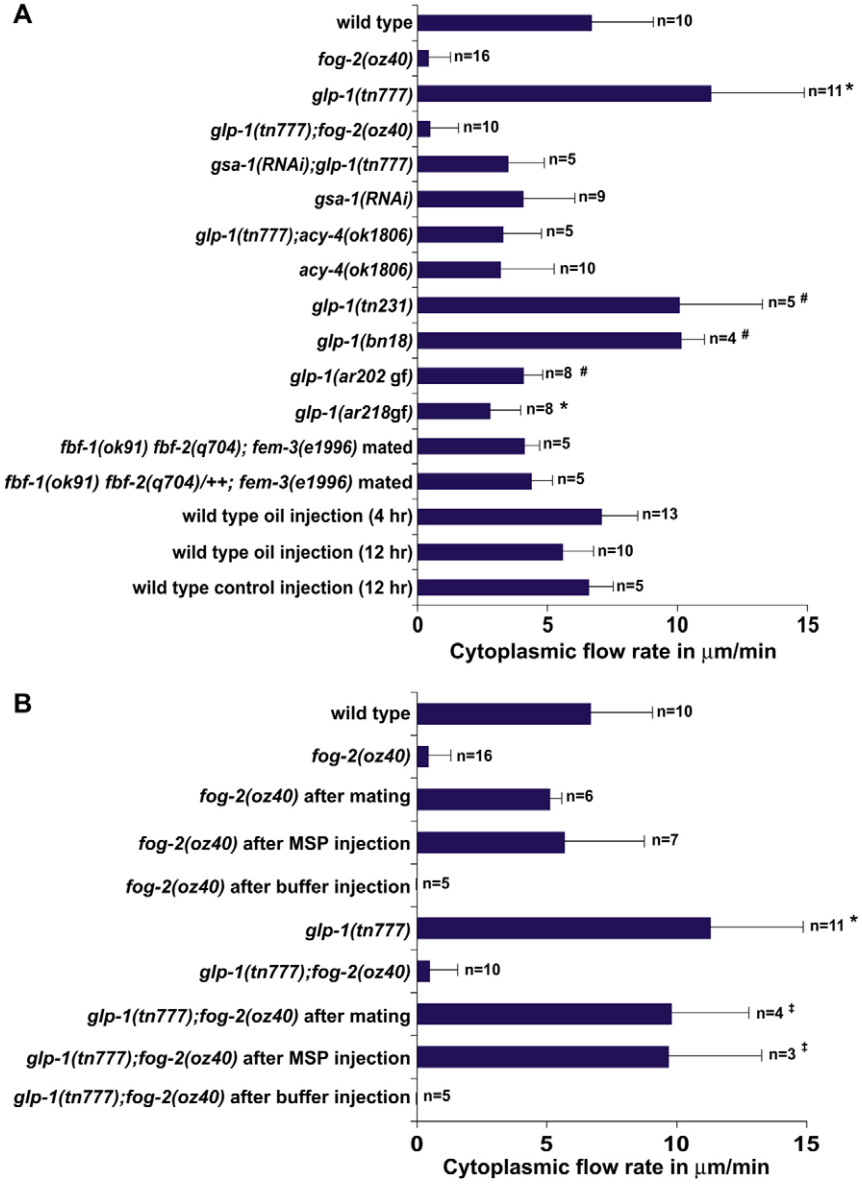

Fig. 4. GLP-1 signaling regulates MSP-dependent cytoplasmic streaming. (**A**) Measurements of cytoplasmic flow rates (DIC particle speed) at 16-20 hours post-L4 in *glp-1* mutant backgrounds. *glp-1(rf)* mutations increase flow; *glp-1(gf)* mutations decrease flow. Flow rates were also analyzed at the same timepoints in the other genetic backgrounds and experimental treatments, except oil injections were also analyzed 12 hours post-injection. (**B**) MSP is sufficient to cause elevated flow rates in *glp-1* mutant females. Hermaphrodites or unmated *fog-2* females were analyzed 1 hour after MSP injection or mating. Flow rates were compared with the wild type: **P*<0.001; #*P*<0.01; ‡*P*<0.05.

glp-1(ts) mutants, we considered the possibility that *glp-1(ts)* mutants might exhibit a distally-extended region of cytoplasmic streaming, but we found this not to be the case (*n*=6). We also found that mating or MSP injection was sufficient to induce elevated cytoplasmic streaming rates in *glp-1* mutant females (Fig. 4B). Elevated cytoplasmic streaming rates in *glp-1* hermaphrodites was dependent on *gsa-1* and *acy-4* (Fig. 4A).

We also observed that proximal oocytes in *glp-1(ts)* mutants retained their connection to the cytoplasmic core for a longer time compared with the wild type (Fig. 5; Table 2). For example, at 16 hours post-L4 at 25°C, the –2 oocyte never remained connected to the cytoplasmic core in the wild type, whereas in *glp-1(tn777ts)* adults the –2 oocyte was connected to the cytoplasmic core in 22-27% of cases (Table 2). Similarly, the –3 oocyte was connected to the cytoplasmic core in 90-100% of *glp-1(tn777ts)* mutants versus 20% in the wild type (Table 2). Since oocytes in *glp-1(tn777ts)* animals mature at ~85% of the wild-type rate, *glp-1* mutant oocytes must retain their connections to the cytoplasmic core for a longer time. *glp-1* mutant oocytes therefore appear to grow large because they receive higher rates of cytoplasmic flow for a longer time period.

Several observations suggest that an elevated flow rate by itself is insufficient to account for the Looc phenotype and that delayed cellularization is a major factor. First, overexpression of ACY-4 from a high-copy array in an *acy-4(lf)* female background results in a markedly increased rate of cytoplasmic streaming (12.9±3.0; *n*=9) (Govindan et al., 2009), but does not cause a Looc phenotype (connection to the cytoplasmic core is not perturbed). Second, mated *fbf-1(ok91) fbf-2(q704); fem-3(e1996)* females did not exhibit elevated cytoplasmic flow rates (Fig. 4A) despite displaying a highly penetrant Looc phenotype (Fig. 1A,B). Like *glp-1(ts)* mutants, proximal oocytes in mated *fbf-1(ok91) fbf-2(q704); fem-3(e1996)* females inappropriately retained their connection to the cytoplasmic core (Table 2). Similarly, distal oil injections did not result in elevated flow (Fig. 4A), however, delays in cellularization were apparent after this treatment (Table 2).

Elevated cytoplasmic streaming and delayed oocyte cellularization in *glp-1* mutants requires gap junction proteins and the *ced-3* and *ced-4* core apoptotic pathway genes

Components of MSP signaling, cell death and MAP kinase pathways have been implicated in cytoplasmic streaming and/or oocyte development, so we examined their interactions with GLP-1 for these phenotypes. Somatic $G\alpha_s$–ACY-4 signaling is necessary and sufficient for sustained cytoplasmic streaming in response to MSP (Govindan et al., 2009), whereas GLP-1 signaling negatively regulates MSP-dependent flow rates (Fig. 4). Thus, we wondered how components of the MSP signaling pathway might interact with the GLP-1 pathway in the regulation of oocyte growth. First we asked whether the *glp-1* oocyte development phenotypes require *inx-22* or *inx-14* function. In the accompanying article, we showed that INX-14 and INX-22 innexin gap junction proteins function in the germline to mediate MSP signaling. Furthermore, we demonstrated a requirement for *inx-14* in promoting germline proliferation or survival (Govindan et al., 2009). We examined the Looc, cytoplasmic flow and oocyte cellularization phenotypes of *glp-1(tn777ts)* in the absence of *inx-22* and found that *inx-22(tm1661)* partially suppressed the Looc phenotype (Fig. 6A,C), completely suppressed the elevated cytoplasmic flow (Fig. 6B), but only partially suppressed the oocyte cellularization defect (Table 2). *inx-14(RNAi)* also suppressed the Looc phenotype of *glp-1(tn777ts)* (Fig. 6A,C) [cytoplasmic flows were not examined using *inx-14(RNAi)*]. The expression pattern of INX-22 in the germline was not affected in *glp-1(tn777ts)* hermaphrodites (S.N. and D.G., unpublished). Next, we examined mutants in *ceh-18*, which encodes a POU-class homeodomain protein required for proper sheath cell differentiation and function that impinges on oocyte development (Rose et al., 1997; Miller et al., 2003). We observed that *ceh-18(mg57)* completely suppressed the elevated cytoplasmic flow rate and partially suppressed the Looc phenotype observed in *glp-1(tn777ts)* hermaphrodites (Fig. 6A-C). The question remained whether an absence of a Looc phenotype in *glp-1(ts)* females was the result of an absence of meiotic maturation. Thus, we examined *goa-1*, which functions as a negative regulator of meiotic maturation (Govindan et al., 2006). Importantly, *goa-1(RNAi)* in a *glp-1(tn777ts); fog-2(oz40)* background did not cause a Looc phenotype, despite exhibiting meiotic maturation (*n*=24). This result indicates that inducing meiotic maturation in a *glp-1* female background is not sufficient to generate a Looc phenotype. We excluded the possibility that *goa-1(RNAi)* suppresses the *glp-1* Looc phenotype or decreases flows in hermaphrodites (Fig. 6A,B). Taken together, these results suggest a complex interconnection between MSP signaling and *glp-1* control of oocyte growth. On the one hand, the MSP meiotic maturation signal is sufficient to induce the Looc phenotype in *glp-1(ts)* females, but on the other hand, three negative regulators of meiotic maturation (*inx-14*, *inx-22* and *ceh-18*) are required for full expression of the *glp-1* mutant Looc phenotype.

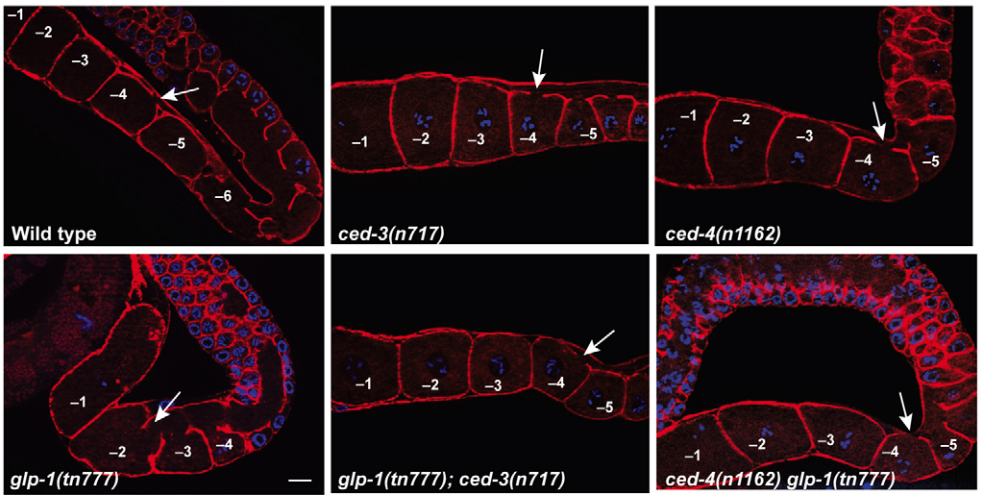

Fig. 5. *glp-1* affects oocyte cellularization. Fluorescence images showing cortical actin staining (red) to visualize the connection of proximal oocytes to the cytoplasmic core. DNA is blue. Animals of the indicated genotypes were examined 16 hours post-L4. Arrow indicates the most proximal oocyte connected to the core. Scale bar: 10 μm.

Table 2. Delayed oocyte cellularization in *glp-1(ts)* mutants

Genotype/experimental treatment*	Method† (*n*)	Oocytes connected to the cytoplasmic core (%)					
		–1	–2	–3	–4	–5	–6
Wild type	F (15)	0	0	20	100	100	100
glp-1(tn777ts)	F (17)	0	27.0	90.0	100	100	100
glp-1(tn777ts); ced-3(n717)	F (15)	0	0	33.3	93.3	100	100
ced-3(n717)	F (19)	0	0	25.0	94.7	100	100
glp-1(tn777ts) ced-4(n1162)	F (15)	0	0	33.3	86.6	100	100
ced-4(n1162)	F (21)	0	0	28.0	90.4	100	100
OD95 P*pie-1-gfp::PH* control	F (12)	0	0	0	25.0	75.0	100
OD95 P*pie-1-gfp::PH* distal oil injection	F (8)	0	62.5	75.0	100	100	100
Wild type	DIC (9)	0	0	22.2	100	100	100
glp-1(tn777ts)	DIC (11)	9.0	22.2	100	100	100	100
fbf-1(ok91) fbf-2(q704); fem-3(e1996) mated	DIC (8)	25.0	75.0	100	100	100	100
fbf-1(ok91) fbf-2(q704)/++; fem-3(e1996) mated	DIC (11)	0	9.0	27.2	72.7	100	100
inx-22(tm1661); glp-1(tn777ts)	DIC (11)	0	9.0	63.6	100	100	100
inx-22(tm1661)	DIC (11)	0	0	27.2	90.9	100	100

*For all strains except OD95, adult hermaphrodites and mated females were examined 16 hours post-L4 to determine which oocytes retained a connection to the cytoplasmic core. OD95 animals were analyzed 24 hours post-injection (~36 hours post-L4).
†Connection of oocytes to the core was analyzed using fluorescence microscopy (F) or functionally using time-lapse DIC microscopy (DIC; oocytes were scored as being connected if they received flow). Fluorescence microscopy was as shown in Fig. 5, except for OD95, in which the GFP::PH plasma membrane marker was used.

Because apoptosis of female meiotic germ cells has been proposed to remove nurse cells, which might contribute cytoplasm to developing oocytes, we investigated the involvement of the cell death pathway in *glp-1* regulation of oocyte growth. Previous results showed that blocking apoptosis of female germ cells with the *ced-3(n717)* mutation does not markedly affect cytoplasmic streaming in the *ced-1(e1735)* background (Wolke et al., 2007), which is also defective in the engulfment of apoptotic corpses. We confirmed that apoptosis is not required for cytoplasmic streaming; *ced-3(n717)* hermaphrodites exhibited normal flow rates (Fig. 6B). The *ced-3(n717)* mutation, which blocks apoptosis, does not reduce oocyte size on the first two days of adulthood (S.N. and D.G., unpublished), however, old *ced-3(n717)* hermaphrodites can contain small abnormal oocytes (Gumienny et al., 1999; Andux and Ellis, 2008). Because apoptosis of female meiotic germ cells has been proposed to remove nurse cells (Gumienny et al., 1999), we examined the effect of *glp-1(tn777ts)* on germline apoptosis using SYTO 12 staining. We observed that germline apoptosis was slightly, but significantly, elevated in *glp-1(tn777ts)* mutants [2.4±1.3 corpses in the wild type, as compared with 3.6±1.9 in *glp-1(tn777ts)*; n=33; P<0.01]. This slight elevation in cell death is unlikely to explain the Looc phenotype because other mutants with elevated germline cell death do not exhibit a Looc phenotype (Navarro et al., 2001; Schumacher et al., 2005). Thus, we were surprised to find that the *ced-3(n717)* and *ced-4(n1162)* mutations strongly suppressed the *glp-1* Looc phenotype (Fig. 6A,C). Both *ced-3(n717)* and *ced-4(n1162)* suppressed the elevated cytoplasmic flow and the delayed oocyte cellularization observed in *glp-1(ts)* mutants (Fig. 5; Fig. 6B; Table 2). By contrast, *cep-1(ep347),* which encodes a p53 homolog required for DNA damage-induced apoptosis in the germline (Derry et al., 2001; Schumacher et al., 2001), did not suppress the *glp-1* Looc phenotype (Fig. 6A). The mechanism by which blocking apoptosis in the germline strongly suppresses all *glp-1* mutant oocyte development phenotypes remains to be determined.

MPK-1 MAPK is also required for normal oocyte growth; *mpk-1(ga111ts)* hermaphrodites exhibit a Looc phenotype (Lee et al., 2007; Arur et al., 2009). We analyzed *mpk-1(ga111ts) glp-1(tn777ts)* double mutants in time-course studies and observed phenotypic enhancement (Fig. 6C,D). Because *mpk-1(ga111ts)* animals do not exhibit elevated flow rates (Fig. 6B), we interpret this enhancement as indicating that GLP-1 and MPK-1 function in parallel. We also observed that the weak gain-of-function *let-60/ras(n1046gf)* mutation strongly suppressed the Looc phenotype and elevated flow rate of *glp-1(tn777ts)* mutants (Fig. 6A-C). Importantly, *let-60/ras(n1046gf)* does not suppress the *glp-1* meiotic entry defect (see Fig. S2 in the supplementary material); thus, *glp-1* regulation of oocyte growth is functionally separable from the meiotic entry defect.

MSP signaling triggers rMLC phosphorylation

To address the mechanism by which MSP and GLP-1 signaling regulate actomyosin-dependent cytoplasmic streaming, we examined the phosphorylation of the MLC-4 regulatory light chain (rMLC) of NMY-2 non-muscle myosin (Jenkins et al., 2006). Phosphorylation of rMLC increases the ATPase activity of non-muscle myosin and is required for myosin motor function, which is needed for cytoplasmic streaming (Wolke et al., 2007). We observed phosphorylated rMLC (P-rMLC) localizing with the cortical actin cytoskeleton throughout the germline where NMY-2 is enriched (Fig. 7A; see Fig. S4 in the supplementary material). P-rMLC was also detected in the gonadal sheath cells (Fig. 7A). The presence of P-rMLC in the germline of unmated females mirrored the MSP requirement for cytoplasmic streaming: young females (less than 16 hours post-L4 at 25°C) that exhibit MSP-independent flow (Govindan et al., 2009) had low levels of P-rMLC (see Fig. S4 in the supplementary material); whereas flows (Govindan et al., 2009) and P-rMLC were not observed in older females (more than 20 hours post-L4; Fig. 7B). P-rMLC is not observed in the gonadal sheath cells of unmated females at any stage (J.A.G. and D.G., unpublished). MSP injection into the uterus of unmated females (30 hours post-L4) rapidly restored P-rMLC throughout the germline within 15 minutes of injection (Fig. 7C), even before meiotic maturation and ovulation occurred. P-rMLC throughout the germline is dependent on $G\alpha_s$–ACY-4 signaling (see Fig. S4 in the supplementary material). Expression of ACY-4 from a high-copy array (*tnEx37*) in an *acy-4(lf)* female background resulted in elevated flow rates (see above). We examined *acy-4(ok1806); tnEx37* females and observed P-rMLC staining in the absence of MSP (see Fig. S4 in the supplementary material). Because genetic mosaic analysis demonstrates that *acy-4* functions in the gonadal

sheath cells and because high-copy arrays are typically silenced in the germline, we conclude that $G\alpha_s$–ACY-4 signaling in sheath cells is necessary and sufficient for phosphorylation of rMLC and for sustained cytoplasmic streaming.

To investigate further the role of P-rMLC in MSP-dependent cytoplasmic streaming, we examined two additional backgrounds in which elevated flow rates are observed: *mel-11(RNAi)* and *glp-1(rf)* mutants. *mel-11* encodes a phosphatase that negatively regulates rMLC phosphorylation (Piekny and Mains, 2002). *mel-11(RNAi)* of wild-type hermaphrodites increased cytoplasmic flow rates to 13.9±3.1 μm/minute (n=5) and resulted in an increase in P-rMLC throughout the germline (see Fig. S5 in the supplementary material). By contrast, in the *glp-1(ts)* background, we observed normal levels of P-rMLC at 25°C (Fig. 7D). Thus,

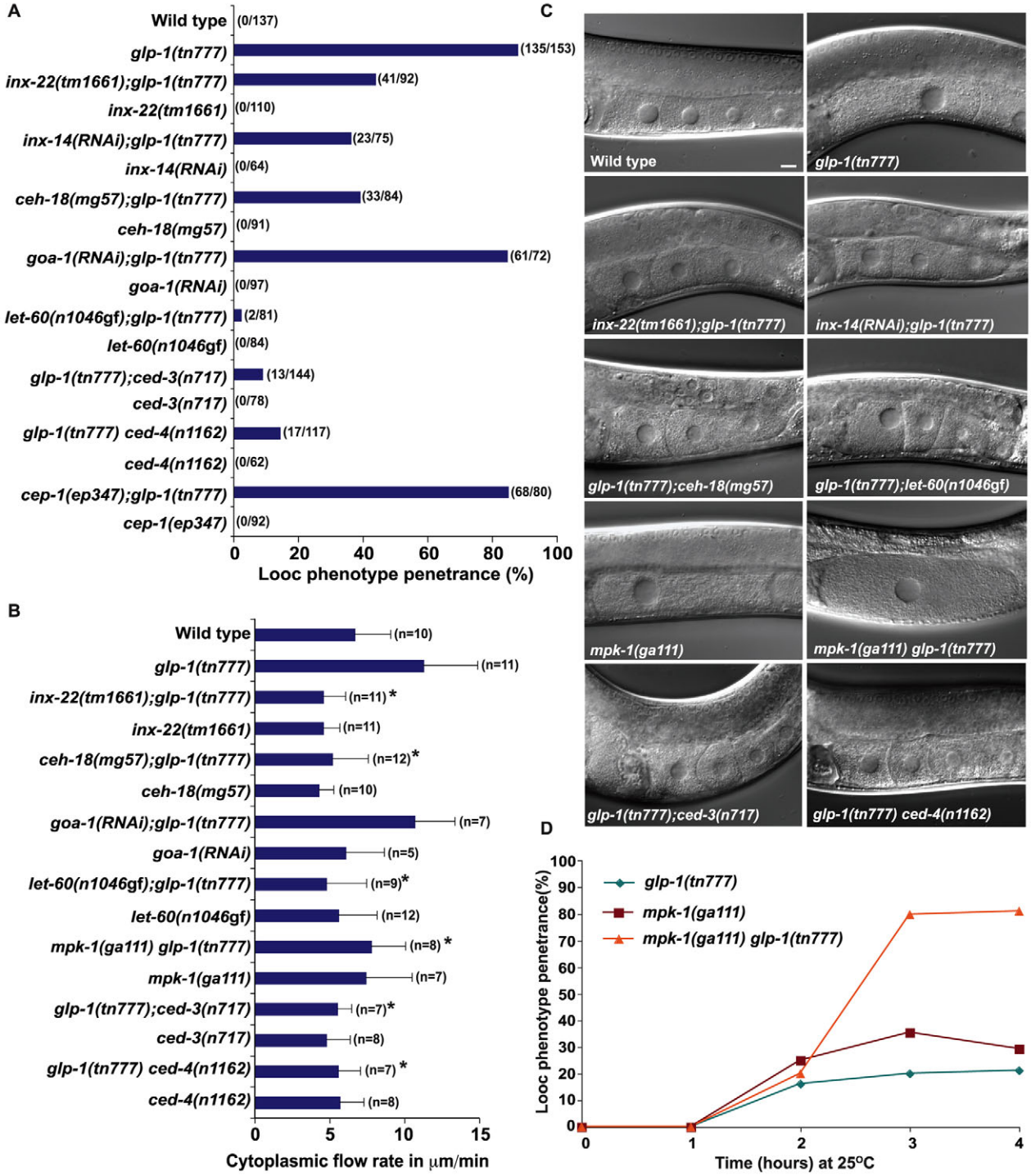

Fig. 6. *glp-1* control of MSP-dependent oocyte growth and cytoplasmic streaming involves gap junction proteins and germ cell apoptosis. (**A-D**) Genetic epistasis analysis of *glp-1(ts)* oocyte growth defects. Looc penetrance (A and D), cytoplasmic flow rates (B) and DIC phenotypes (C) were analyzed. Because *mpk-1(ga111ts)* causes severe gonad disorganization after transfer to 25°C for prolonged periods, day-1 adults were shifted and analyzed within 4 hours. **P*<0.0005 in comparison to *glp-1(tn777ts)*. Scale bar: 10 μm.

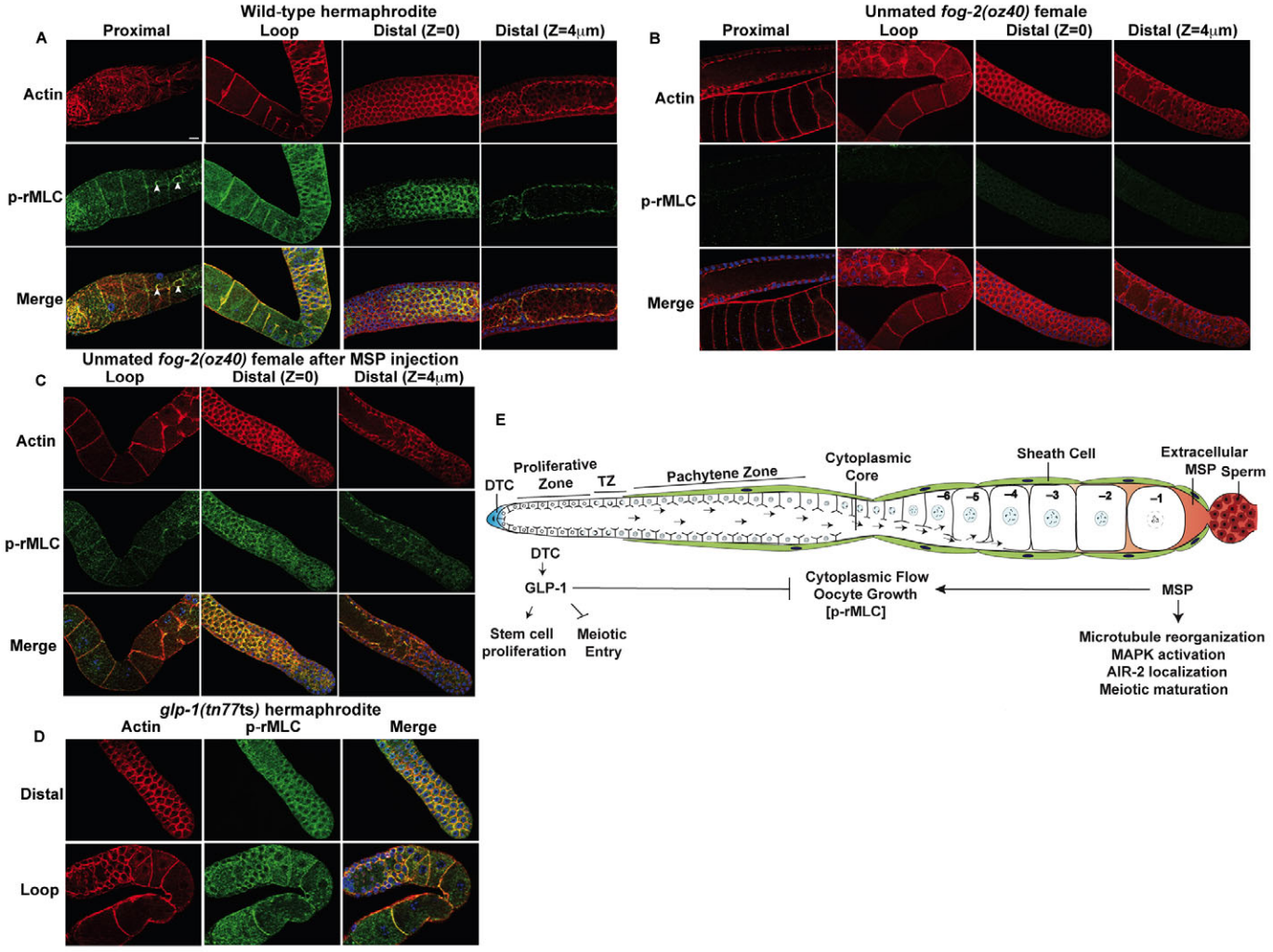

Fig. 7. MSP signaling triggers rMLC phosphorylation throughout the gonad arm. (**A-D**) Detection of cortical actin (red) and P-rMLC using PSer19-MLC antibodies (green) in dissected gonads from hermaphrodites (A), unmated *fog-2(oz40)* females (B), MSP-injected *fog-2(oz40)* females 15 minutes post-injection (C) and *glp-1(tn777ts)* hermaphrodites (D). Arrowheads indicate P-rMLC staining in ring channels of the proximal oocytes. DNA is blue. Scale bar: 10 μm. (**E**) A model for the control of germline proliferation, oocyte growth and meiotic maturation by GLP-1 and MSP signaling (see text for details). P-rMLC is shown in brackets to indicate that MSP signaling is sufficient to promote rMLC phosphorylation in the germline, whereas the *glp-1* pathway appears dispensable.

MSP signaling can affect cytoplasmic streaming by two mechanisms: one involving rMLC phosphorylation and a second modulated by GLP-1 signaling.

DISCUSSION

We show that GLP-1/Notch signaling restricts the growth of oocytes to the proper size in response to the MSP signal. Germline GLP-1 activity negatively regulates MSP-dependent cytoplasmic streaming and oocyte cellularization. Several observations suggest that GLP-1 functions in the distal germline in response to DTC signaling to regulate oocyte growth. Laser ablation of the DTC and co-depletion of the DTC-expressed GLP-1 ligands LAG-2 and APX-1 cause a Looc phenotype. Furthermore, disruption of the proliferative zone via oil injection causes oocytes to grow abnormally large. Although this operation affects the proliferative zone, proximal germ cells appear morphologically normal and fertility is retained. Distal oil injection not only suppresses the small oocyte phenotype of *glp-1(ar202gf)*, but produces a *glp-1(rf)* phenocopy. Normal oocyte growth requires the function of several mediators of GLP-1 signaling, including the LAG-1 transcription factor and the FBF-1/2 RNA-binding proteins. We note that the distribution of GLP-1-INTRA is unknown. Furthermore, APX-1 is also expressed in proximal gonadal sheath cells (M.M. and E.J.A.H., unpublished). Therefore, although we cannot formally exclude a proximal role for GLP-1 activity, the data are most consistent with a model in which activation of GLP-1 signaling in the distal germline triggers events that culminate in the regulation of oocyte growth, preventing overgrowth of oocytes.

Are the effects of *glp-1* on oocyte growth an indirect consequence of defects in the proliferation versus meiotic entry decision?

In response to signals from the DTC, GLP-1 activity promotes the proliferation of the distal stem cell population and/or inhibits their meiotic entry (Kimble and Crittenden, 2007). DTC signaling is also required for *glp-1*-dependent activities that restrict oocyte growth. One hypothesis to explain this unexpected observation is that the large oocyte phenotype occurs as a consequence of defects in the

proliferation versus meiotic entry decision of distal germ cells. Several observations argue against this hypothesis and, instead, suggest that the role of *glp-1* in oocyte growth is separable from the proliferation versus meiotic entry decision. First, the Looc phenotype is manifest in a much shorter timeframe than that required for the majority of germ cells to enter meiosis. Nor do Looc mutants contain an overabundance of pachytene nuclei, ruling out the possibility that increased flows and large oocytes result from additional pachytene nuclei (see Table S1 in the supplementary material). Second, germline stem cells enter meiosis upon upshift of *glp-1(ts)* alleles in both the presence and absence of sperm, whereas the Looc phenotype is sperm-dependent. Third, blocking apoptosis of pachytene-stage meiotic germ cells strongly suppresses the *glp-1* oocyte growth defect without affecting the premature meiotic entry defect. It is not clear whether the *ced-3* and *ced-4* requirement for the *glp-1* Looc phenotype involves their essential role in apoptosis, or whether it might reflect a cell death-independent function (Yi and Yuan, 2009). Fourth, inactivation of the germline innexins *inx-14* and *inx-22* specifically suppresses the *glp-1* Looc phenotype. Finally, in *glp-1(tn777ts); let-60/ras(n1046gf)* double mutants, all germ cells enter meiosis and all aspects of the *glp-1* Looc phenotype (i.e. elevated flows and delayed cellularization) are strongly suppressed. Nevertheless, without the identification of relevant direct targets of GLP-1, we cannot exclude the formal possibility that cell fate changes in the distal germline in *glp-1* mutants affect oocyte growth. Interestingly, mated *fbf-1(ok91) fbf-2(q704); fem-3(e1996)* females exhibit delayed oocyte cellularization but normal flow rates, and the same effect is observed after distal oil injections. Thus, the negative regulation of cytoplasmic streaming and positive regulation of oocyte cellularization might be further separable responses to *glp-1* activity. One possibility is that a transcriptional target protein of GLP-1 signaling is transported proximally in the cytoplasmic core where it functions to modulate cytoplasmic flow.

A related issue is whether the large oocyte phenotype in *glp-1(rf)* mutants occurs as a direct consequence of the meiotic entry of distal germ cells. A time-course analysis of the *glp-1* requirement for normal oocyte growth revealed that ~20% of *glp-1(ts)* germlines showed a Looc phenotype with 2 hours of upshift (Fig. 2), prior to a significant increase in meiotic entry. This finding argues against the Looc phenotype being a direct consequence of meiotic entry of all germ cells in the distal germline. However, the penetrance of the Looc phenotype increases slowly in this experiment and reaches its maximum value (~80%) after 8 hours, when all germ cells have entered meiosis following the *glp-1(ts)* upshift. Thus, it remains possible that at least some portion of the Looc phenotype in *glp-1(rf)* backgrounds is a direct cell biological consequence of meiotic entry of all germ cells in the distal germline.

A model for the coordinate control of oogenesis by MSP and GLP-1 signaling

The results presented here support a model in which two major signaling centers in the adult hermaphrodite gonad, distal GLP-1 signaling and proximal MSP signaling, work in opposition to regulate the differentiation of germ cells into functional oocytes (Fig. 7E). In this model, the adult hermaphrodite gonad is rapidly switched into a reproductive mode by the MSP hormone. MSP signaling provides the impetus for oocyte growth, differentiation and the completion of meiosis, and GLP-1 signaling both provides the raw material for gametogenesis and modulates additional processes that restrict oocyte growth. $G\alpha_s$–ACY-4 signaling in the gonadal sheath cells is required for all described MSP responses in the germline (Govindan et al., 2009) (and this work). The gonadal sheath cells form gap junctions with each other and with the germline, providing a mechanism by which the gonadal sheath cells might widely communicate the presence of MSP. MSP rapidly induces cytoplasmic streaming and rMLC phosphorylation as far as the proliferative zone. In turn, DTC signaling ensures a proper growth response to MSP, in effect licensing stem cells for differentiation, fertilization and embryogenesis. In this model, GLP-1 produces regulators of oocyte growth, the effects of which require MSP signaling. Notch signaling might similarly regulate long-range cytoplasmic transport in vertebrate systems. By regulating intracellular transport, Notch signaling might operate over short distances to establish polarity within a cell. Likewise, Notch signaling might modulate responses to MSP-related ligands (Tsuda et al., 2008) in mammals. Thus, the findings reported here might have wider implications for the regulation of intercellular signaling, beyond the scope of the *C. elegans* germline.

We are grateful to the *Caenorhabditis* Genetics Center, Anjon Audhya, Dave Hansen and Tim Schedl for providing strains and reagents. Thanks to Ikuko Yamamoto, Tokiko Furuta and John Maciejowski for technical assistance; Mary Montgomery generously shared her laser ablation set up. We especially thank Bob Herman, Tim Schedl, Geraldine Seydoux and John Yochem for helpful suggestions and experimental advice. Hua Cheng, Dave Hansen, Bob Herman, Seongseop Kim, Ann Rougvie, Caroline Spike, Todd Starich and John Yochem provided comments on the manuscript. This work was supported by NIH grants GM65115 and GM57173 to D.G. and GM61706 to J.H. Deposited in PMC for release after 12 months.

Supplementary material

Supplementary material for this article is available at
http://dev.biologists.org/cgi/content/full/136/13/2223/DC1

References

Andux, S. and Ellis, R. E. (2008). Apoptosis maintains oocyte quality in aging *Caenorhabditis elegans* females. *PLoS Genet.* **4**, e1000295.
Arur, S., Ohmachi, M., Nayak, S., Hayes, M., Miranda, A., Hay, A., Golden, A. and Schedl, T. (2009). Functional genomic identification of multiple ERK substrates in *Caenorhabditis elegans* germ cell development. *Proc. Natl. Acad. Sci. USA* **106**, 4776-4781.
Austin, J. and Kimble, J. (1987). *glp-1* is required in the germline for regulation of the decision between mitosis and meiosis in *C. elegans*. *Cell* **51**, 589-599.
Austin, J. and Kimble, J. (1989). Transcript analysis of *glp-1* and *lin-12*, homologous genes required for cell interactions during development of *C. elegans*. *Cell* **58**, 565-571.
Chen, N. and Greenwald, I. (2004). The lateral signal for LIN-12/Notch in *C. elegans* vulval development comprises redundant secreted and transmembrane DSL proteins. *Dev. Cell* **6**, 183-192.
Christensen, S., Kodoyianni, V., Bosenberg, M., Friedman, L. and Kimble, J. (1996). *lag-1*, a gene required for *lin-12* and *glp-1* signaling in *Caenorhabditis elegans*, is homologous to human CBF1 and Drosophila Su(H). *Development* **122**, 1373-1383.
Crittenden, S. L., Troemel, E. R., Evans, T. C. and Kimble, J. (1994). GLP-1 is localized to the mitotic region of the *C. elegans* germline. *Development* **120**, 2901-2911.
Crittenden, S. L., Bernstein, D. S., Bachorik, J. L., Thompson, B. E., Gallegos, M., Petcherski, A. G., Moulder, G., Barstead, R., Wickens, M. and Kimble, J. (2002). A conserved RNA-binding protein controls germline stem cells in *Caenorhabditis elegans*. *Nature* **417**, 660-663.
Derry, W. B., Putzke, A. P. and Rothman, J. H. (2001). *Caenorhabditis elegans* p53: role in apoptosis, meiosis, and stress resistance. *Science* **294**, 591-595.
Govindan, J. A., Cheng, H., Harris, J. E. and Greenstein, D. (2006). $G\alpha_{o/i}$ and $G\alpha_s$ signaling function in parallel with the MSP/Eph receptor to control meiotic diapause in *C. elegans*. *Curr. Biol.* **16**, 1257-1268.
Govindan, J. A., Nadarajan, S., Kim, S., Starich, T. A. and Greenstein, D. (2009). Somatic cAMP signaling regulates MSP-dependent oocyte growth and meiotic maturation in *C. elegans*. *Development* **136**, 2211-2221.
Grant, B. and Hirsh, D. (1999). Receptor-mediated endocytosis in the *Caenorhabditis elegans* oocyte. *Mol. Biol. Cell* **10**, 4311-4326.
Gumienny, T. L., Lambie, E., Hartwieg, E., Horvitz, H. R. and Hengartner, M. O. (1999). Genetic control of programmed cell death in the *Caenorhabditis elegans* hermaphrodite germline. *Development* **126**, 1011-1022.
Gutch, M. J., Flint, A. J., Keller, J., Tonks, N. K. and Hengartner, M. O. (1998). The *Caenorhabditis elegans* SH2 domain-containing protein tyrosine phosphatase PTP-2 participates in signal transduction during oogenesis and vulval development. *Genes Dev.* **12**, 571-585.

Hansen, D. and Schedl, T. (2006). The regulatory network controlling the proliferation-meiotic entry decision in the *Caenorhabditis elegans* germline. *Curr. Top. Dev. Biol.* **76**, 185-215.
Hansen, D., Wilson-Berry, L., Dang, T. and Schedl, T. (2004). Control of the proliferation versus meiotic development decision in the *C. elegans* germline through regulation of GLD-1 protein accumulation. *Development* **131**, 93-104.
Hedgecock, E. M. and Herman, R. K. (1995). The *ncl-1* gene and genetic mosaics of *Caenorhabditis elegans*. *Genetics* **141**, 989-1006.
Henderson, S. T., Gao, D., Lambie, E. J. and Kimble, J. (1994). *lag-2* may encode a signaling ligand for the GLP-1 and LIN-12 receptors of *C. elegans*. *Development* **120**, 2913-2924.
Hirsh, D., Oppenheim, D. and Klass, M. (1976). Development of the reproductive system of *Caenorhabditis elegans*. *Dev. Biol.* **49**, 200-219.
Jaramillo-Lambert, A., Ellefson, M., Villeneuve, A. M. and Engebrecht, J. (2007). Differential timing of S phases, X chromosome replication, and meiotic prophase in the *C. elegans* germline. *Dev. Biol.* **308**, 206-221.
Jenkins, N., Saam, J. R. and Mango, S. E. (2006). CYK-4/GAP provides a localized cue to initiate anteroposterior polarity upon fertilization. *Science* **313**, 1298-1301.
Kimble, J. E. and White, J. G. (1981). On the control of germ cell development in *Caenorhabditis elegans*. *Dev. Biol.* **81**, 208-219.
Kimble, J. and Crittenden, S. L. (2007). Controls of germline stem cells, entry into meiosis, and the sperm/oocyte decision in *Caenorhabditis elegans*. *Annu. Rev. Cell Dev. Biol.* **23**, 405-433.
Kodoyianni, V., Maine, E. M. and Kimble, J. (1992). Molecular basis of loss-of-function mutations in the *glp-1* gene of *Caenorhabditis elegans*. *Mol. Biol. Cell* **3**, 1199-1213.
Lambie, E. J. and Kimble, J. (1991). Two homologous regulatory genes, *lin-12* and *glp-1*, have overlapping functions. *Development* **112**, 231-240.
Lamont, L. B., Crittenden, S. L., Bernstein, D., Wickens, M. and Kimble, J. (2004). FBF-1 and FBF-2 regulate the size of the mitotic region in the *C. elegans* germline. *Dev. Cell* **7**, 697-707.
Lee, M. H., Ohmachi, M., Arur, S., Nayak, S., Francis, R., Church, D., Lambie, E. and Schedl, T. (2007). Multiple functions and dynamic activation of MPK-1 ERK signaling in *C. elegans* germline development. *Genetics* **177**, 2039-2062.
Maddox, A. S., Habermann, B., Desai, A. and Oegema, K. (2005). Distinct roles for two *C. elegans* anillins in the gonad and early embryo. *Development* **132**, 2837-2848.
McCarter, J., Bartlett, B., Dang, T. and Schedl, T. (1999). On the control of oocyte meiotic maturation and ovulation in *C. elegans*. *Dev. Biol.* **205**, 111-128.
Mello, C. C., Draper, B. W. and Priess, J. R. (1994). The maternal genes *apx-1* and *glp-1* and establishment of dorsal-ventral polarity in the early *C. elegans* embryo. *Cell* **77**, 95-106.
Miller, M. A., Nguyen, V. Q., Lee, M. H., Kosinski, M., Schedl, T., Caprioli, R. M. and Greenstein, D. (2001). A sperm cytoskeletal protein that signals oocyte meiotic maturation and ovulation. *Science* **291**, 2144-2147.
Miller, M. A., Ruest, P. J., Kosinski, M., Hanks, S. K. and Greenstein, D. (2003). An Eph receptor sperm-sensing control mechanism for oocyte meiotic maturation in *Caenorhabditis elegans*. *Genes Dev.* **17**, 187-200.
Navarro, R. E., Shim, E. Y., Kohara, Y., Singson, A. and Blackwell, T. K. (2001). *cgh-1*, a conserved predicted RNA helicase required for gametogenesis and protection from physiological germline apoptosis in *C. elegans*. *Development* **128**, 3221-3232.
Piekny, A. J. and Mains, P. E. (2002). Rho-binding kinase (LET-502) and myosin phosphatase (MEL-11) regulate cytokinesis in the early *Caenorhabditis elegans* embryo. *J. Cell Sci.* **115**, 2271-2282.
Priess, J. R., Schnabel, H. and Schnabel, R. (1987). The *glp-1* locus and cellular interactions in early *C. elegans* embryos. *Cell* **51**, 601-611.
Rose, K. L., Winfrey, V. P., Hoffman, L. H., Hall, D. H., Furuta, T. and Greenstein, D. (1997). The POU gene *ceh-18* promotes gonadal sheath cell differentiation and function required for meiotic maturation and ovulation in *Caenorhabditis elegans*. *Dev. Biol.* **192**, 59-77.
Schedl, T. (1997). Developmental genetics of the germline. In *C. elegans II* (ed. D. Riddle, T. Blumenthal, B. Meyer and J. Priess), pp. 241-270. Cold Spring Harbor, NY: Cold Spring Harbor Laboratory Press.
Schumacher, B., Hofmann, K., Boulton, S. and Gartner, A. (2001). The *C. elegans* homolog of the p53 tumor suppressor is required for DNA damage-induced apoptosis. *Curr. Biol.* **11**, 1722-1727.
Schumacher, B., Hanazawa, M., Lee, M. H., Nayak, S., Volkmann, K., Hofmann, E. R., Hengartner, M., Schedl, T. and Gartner, A. (2005). Translational repression of *C. elegans* p53 by GLD-1 regulates DNA damage-induced apoptosis. *Cell* **120**, 357-368.
Shelton, C. A., Carter, J. C., Ellis, G. C. and Bowerman, B. (1999). The nonmuscle myosin regulatory light chain gene *mlc-4* is required for cytokinesis, anterior-posterior polarity, and body morphology during *Caenorhabditis elegans* embryogenesis. *J. Cell Biol.* **146**, 439-451.
Sijen, T., Fleenor, J., Simmer, F., Thijssen, K. L., Parrish, S., Timmons, L., Plasterk, R. H. and Fire, A. (2001). On the role of RNA amplification in dsRNA-triggered gene silencing. *Cell* **107**, 465-476.
Swan, K. A., Severson, A. F., Carter, J. C., Martin, P. R., Schnabel, H., Schnabel, R. and Bowerman, B. (1998). *cyk-1*: a *C. elegans* FH gene required for a late step in embryonic cytokinesis. *J. Cell Sci.* **111**, 2017-2027.
Tax, F. E., Yeargers, J. J. and Thomas, J. H. (1994). Sequence of *C. elegans lag-2* reveals a cell-signalling domain shared with Delta and Serrate of Drosophila. *Nature* **368**, 150-154.
Thompson, B. E., Bernstein, D. S., Bachorik, J. L., Petcherski, A. G., Wickens, M. and Kimble, J. (2005). Dose-dependent control of proliferation and sperm specification by FOG-1/CPEB. *Development* **132**, 3471-3481.
Tsuda, H., Han, S. M., Yang, Y., Tong, C., Lin, Y. Q., Mohan, K., Haueter, C., Zoghbi, A., Harati, Y., Kwan, J. et al. (2008). The amyotrophic lateral sclerosis 8 protein VAPB is cleaved, secreted, and acts as a ligand for Eph receptors. *Cell* **133**, 963-977.
Wolke, U., Jezuit, E. A. and Priess, J. R. (2007). Actin-dependent cytoplasmic streaming in *C. elegans* oogenesis. *Development* **134**, 2227-2236.
Yi, C. H. and Yuan, J. (2009). The Jekyll and Hyde functions of caspases. *Dev. Cell* **16**, 21-34.
Yochem, J. and Greenwald, I. (1989). *glp-1* and *lin-12*, genes implicated in distinct cell-cell interactions in *C. elegans*, encode similar transmembrane proteins. *Cell* **58**, 553-563.
Zhang, B., Gallegos, M., Puoti, A., Durkin, E., Fields, S., Kimble, J. and Wickens, M. P. (1997). A conserved RNA-binding protein that regulates sexual fates in the *C. elegans* hermaphrodite germline. *Nature* **390**, 477-484.

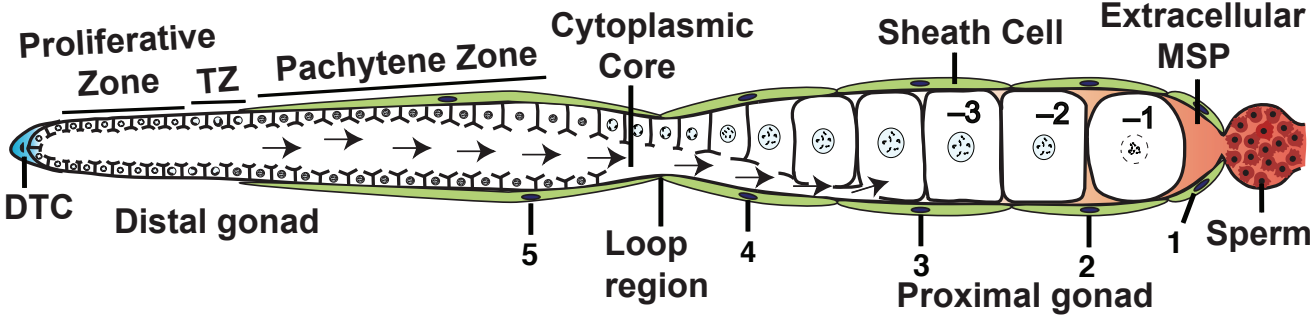
Proliferative Zone
TZ
Pachytene Zone
Cytoplasmic Core
Sheath Cell
Extracellular MSP
–3
–2
–1
DTC
Distal gonad
5
Loop region
4
3
2
1
Sperm
Proximal gonad

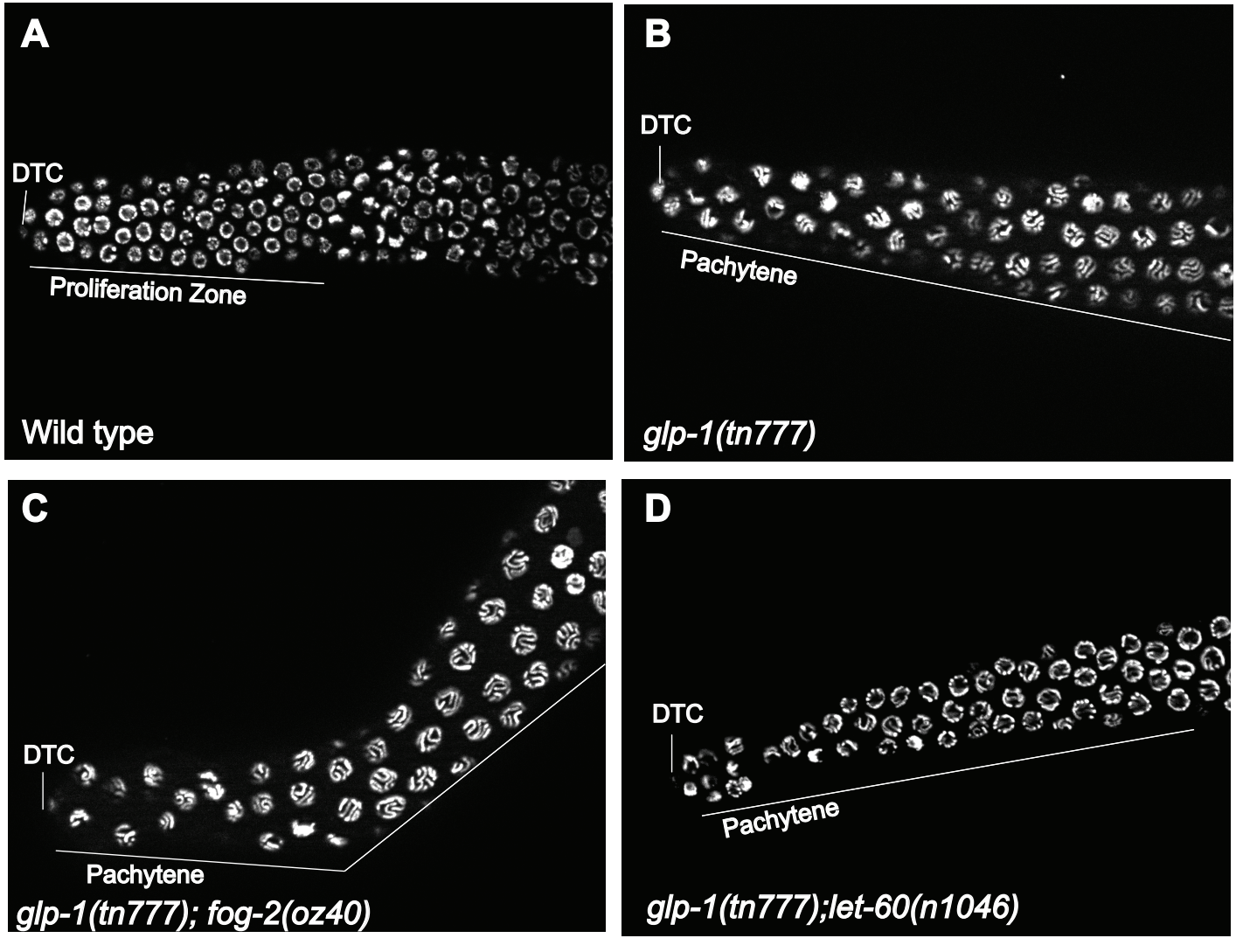
A
DTC
Proliferation Zone
Wild type
B
DTC
Pachytene
glp-1(tn777)
C
DTC
Pachytene
glp-1(tn777); fog-2(oz40)
D
DTC
Pachytene
glp-1(tn777);let-60(n1046)

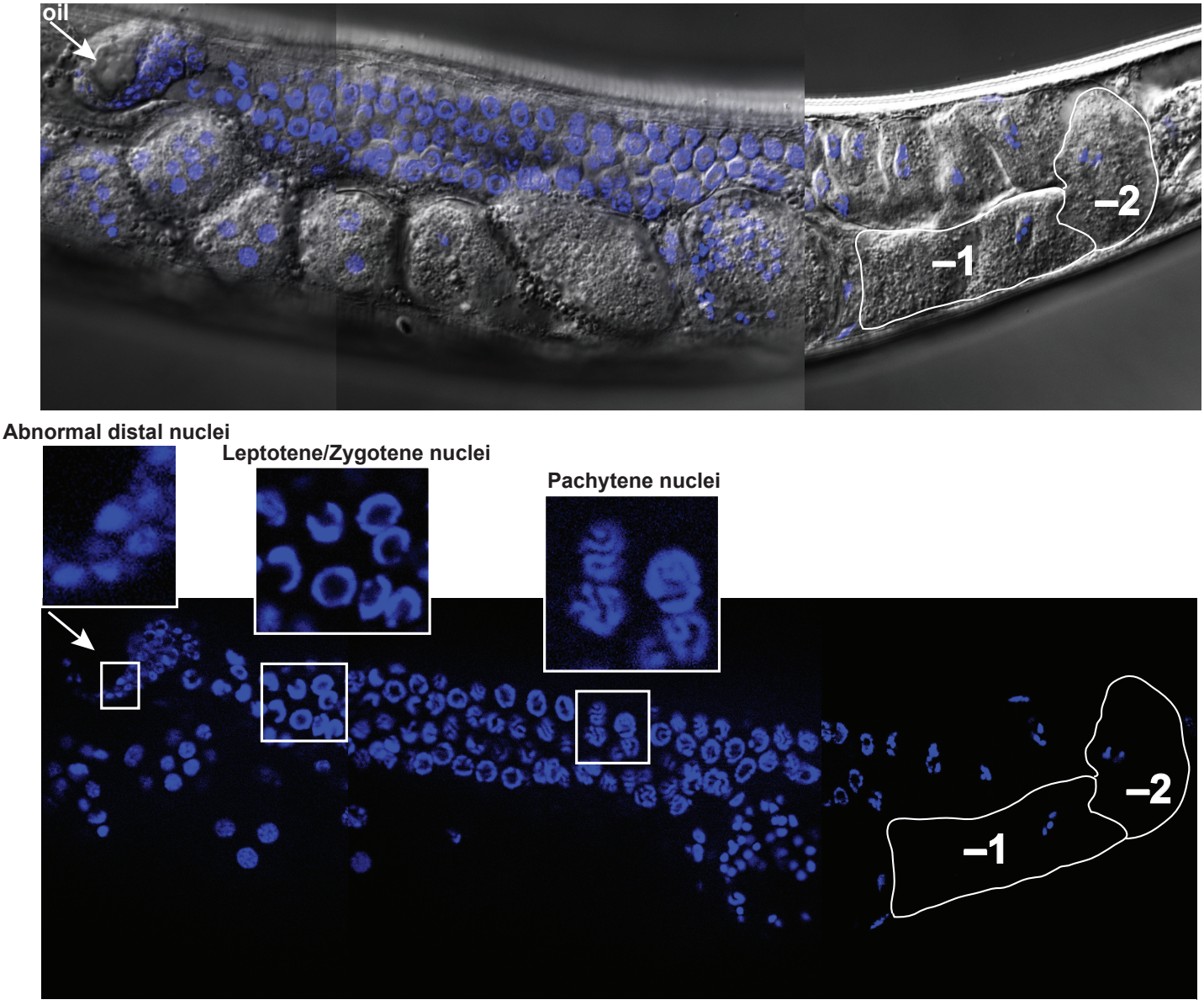
oil
–2
–1
Abnormal distal nuclei
Leptotene/Zygotene nuclei
Pachytene nuclei
–2
–1

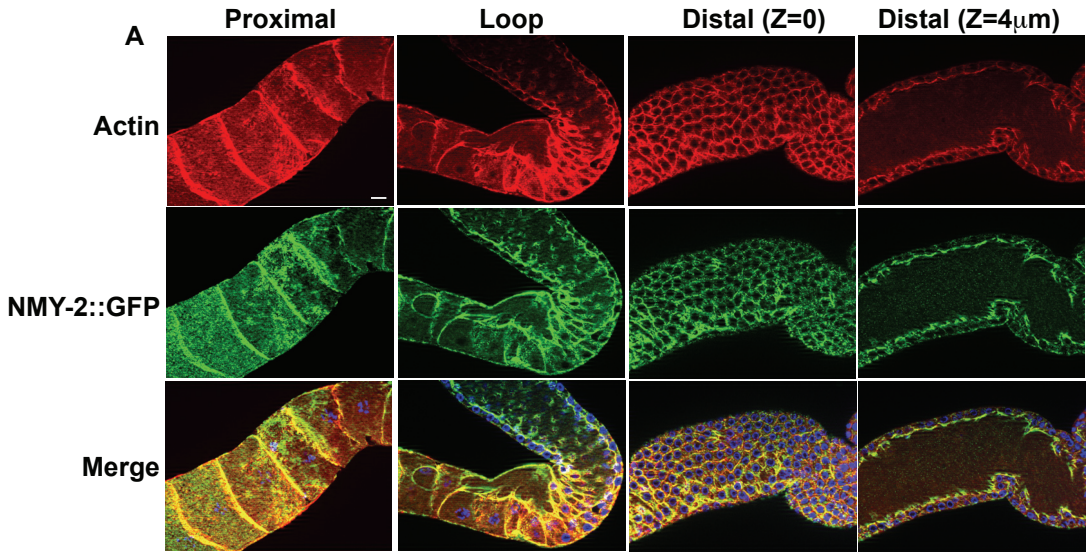
A
Proximal
Loop
Distal (Z=0)
Distal (Z=4μm)
Actin
NMY-2::GFP
Merge

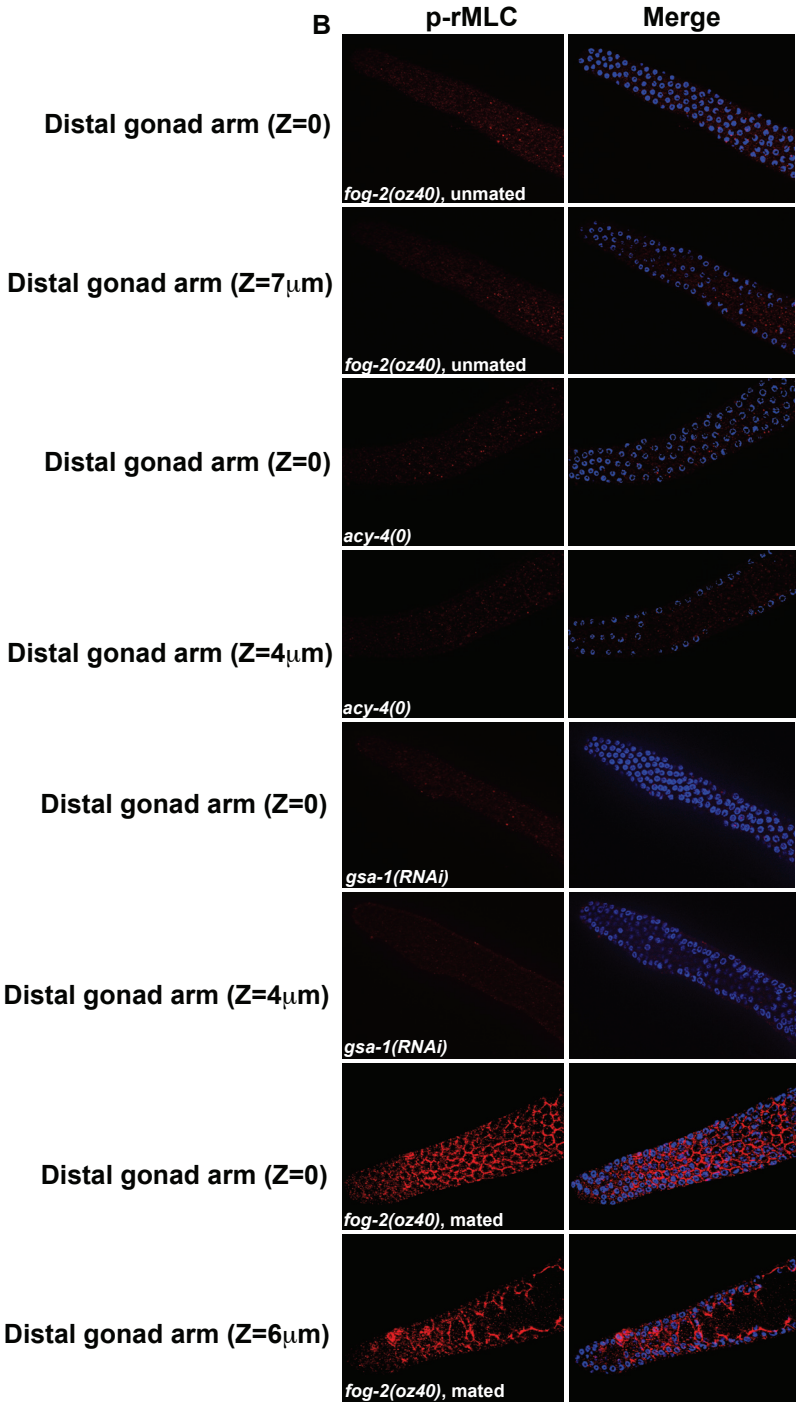
B
p-rMLC
Merge
Distal gonad arm (Z=0)
fog-2(oz40), unmated
Distal gonad arm (Z=7μm)
fog-2(oz40), unmated
Distal gonad arm (Z=0)
acy-4(0)
Distal gonad arm (Z=4μm)
acy-4(0)
Distal gonad arm (Z=0)
gsa-1(RNAi)
Distal gonad arm (Z=4μm)
gsa-1(RNAi)
Distal gonad arm (Z=0)
fog-2(oz40), mated
Distal gonad arm (Z=6μm)
fog-2(oz40), mated

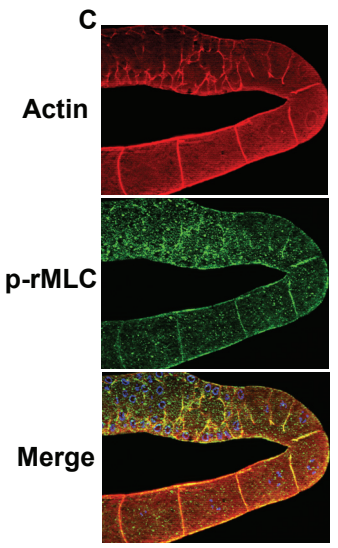
C
Actin
p-rMLC
Merge

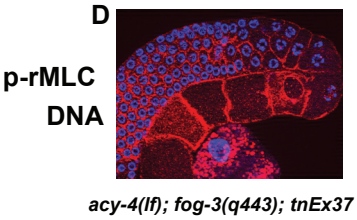
D
p-rMLC
DNA
acy-4(lf); fog-3(q443); tnEx37

A

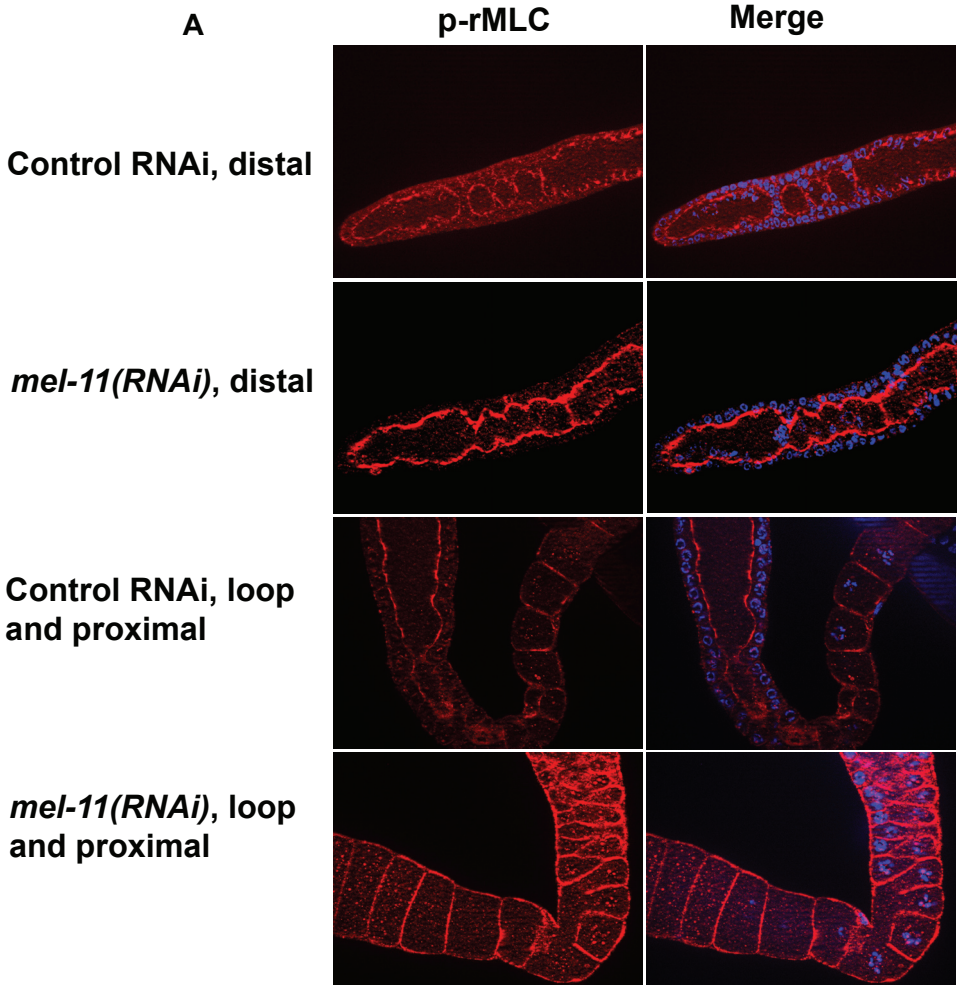

B

	Quantification of p-rMLC staining in arbitrary fluorescence units	
	Control RNAi	*mel-11(RNAi)*
Distal	41.46 ± 6.94 (5)	79.91 ± 8.06 (5)*
Loop	29.55 ± 6.01 (5)	44.38 ± 13.17 (6)#
Proximal	32.92 ± 9.02(5)	51.44 ± 12.60 (7)‡

Table S1. *glp-1(tn777ts)* mutants do not contain excess pachytene cells

	Classification of germ cell morphology using DAPI staining			
Genotype	Proliferation	Transition	Pachytene	*n*
Wild type	180±36	85±33	297±57	20
glp-1(tn777ts)	0	16±9	131±34	21
fog-2(oz40)	151±39	44±7	234±37	17
glp-1(tn777ts); fog-2(oz40)	0	24±14	154±22	18

L4 larvae of the indicated genotypes were transferred from 15°C to 25°C and the cytology of germ cells was analyzed in fixed and DAPI-stained dissected gonad preparations at 16 hours post-L4. Photographic images of a *z*-series of each gonad arm were taken and the germ cells were counted and classified (diplotene, diakinesis are not presented here).

Table S2. Redundant requirement of *lag-2* and *apx-1* for germline proliferation

Background and phenotype*	RNAi†	%	*n*‡
Wild type	Control	–	307
0	–	0	–
1-10	–	0	–
11-40	–	0	–
>50, <200	–	0	–
Wild type	*apx-1*	–	94
0	–	0	–
1-10	–	0	–
11-40	–	0	–
>50, <200	–	16	–
lag-2(q420ts)	Control	–	50
0	–	35	–
1-10	–	0	–
11-40	–	6	–
>50, <200	–	39	–
lag-2(q420ts)	*apx-1*	–	26
0	–	58	–
1-10	–	0	–
11-40	–	8	–
>50, <200	–	38	–
apx-1(or3)	Control	–	40
0	–	0	–
1-10	–	0	–
11-40	–	0	–
>50, <200	–	5	–
apx-1(or3)	*lag-2*	–	42
0	–	38	–
1-10	–	29	–
11-40	–	14	–
>50, <200	–	17	–

*Gonad arms were classified by the number of nuclei in the proliferative zone (nuclei with non-meiotic morphology, distal to the transition zone). This table reports all classifications of defects observed in the experiment shown in Fig. 3E, which presents only the most severe class (the '0' class or 'Glp-1-like phenotype' in which all germ cells display a nuclear morphology consistent with meiotic prophase or gametogenesis). The last category includes gonad arms in which more than 50 but noticeably fewer than the normal ~200 were observed. Remaining gonad arms were normal.

†For the *apx-1(RNAi)* and controls, to avoid embryonic lethality, RNAi was performed as follows: after rearing strains at 15°C, synchronous L1 larvae were transferred to RNAi plates at 20°C and fixed and stained with DAPI ~50 hours later. For the *lag-2(RNAi)* and controls, conditions were the same except that L4 animals were placed on the appropriate RNAi bacteria, and removed after 1 day, after which the progeny were scored the next day. Control RNAi was the L4440 vector.

‡Number of gonad arms counted.

Table S3. *apx-1* activity influences the number of nuclei in the germline proliferative zone after the L2 stage in a soma-dependent manner

Relevant genotype	Time (hours)*	Average±s.e.m.	*n*†
apx-1(+)			
	17	21±1	36
	24	51±3	24
	31	113±3	39
	41	212±11	13
	48	230±5	14
apx-1(or3)			
	17	20±3	12
	24	68±3	12
	31	98±6	18
	41	166±26	4
	48	171±6	31
Control RNAi			
	19	22±1	2
	48	208±0.5	3
apx-1(RNAi)			
	19	23±0.75	4
	48	120±4	4
rrf-1(pk1417); apx-1(RNAi)			
	24	63±6	16
	48	198±11	16

*Hours post-hatch at 25°C. Gravid adults laid eggs overnight at 25°C, progeny were synchronized as L1 larvae by hatch-off and placed on the appropriate RNAi plates and scored after staining with DAPI.
†Number of gonad arms counted.